Appl. Phys. A 79, 945–948 (2004)
DOI: 10.1007/s00339-004-2576-3

**Applied Physics A**
**Materials Science & Processing**

X.R. ZHANG[1]
X. XU[1,✉]
A.M. RUBENCHIK[2]

# Simulation of microscale densification during femtosecond laser processing of dielectric materials

[1] School of Mechanical Engineering, Purdue University, West Lafayette, IN 47907, USA
[2] Mail stop L399, Lawrence Livermore National Laboratory, Livermore, CA 94550, USA

**Received: 1 October 2003/Accepted: 17 December 2003**
**Published online: 26 July 2004 • © Springer-Verlag 2004**

**ABSTRACT** It has been demonstrated that femtosecond laser pulses can be used to process dielectric materials such as optical glass. One of the applications of this process is to produce sub-diffraction-limit structures whose index of refraction is different from that of the host medium. Due to the small size of these 'bits', it has been proposed to use this technique for high-density optical data storage. This paper is concerned with the mechanisms of the change of the index of refraction in such a small domain. We propose that the laser-induced strain field is responsible for the localized change of the index of refraction. It is demonstrated that the compressive strain field could be smaller than the area where the laser energy is absorbed in the glass.

**PACS** 42.62.-b; 78.20.Hp; 81.40.Lm

## 1 Introduction

Recently, many investigators have demonstrated that, by using femtosecond laser pulses, three-dimensional (3-D) sub-microstructures with modified index of defraction can be written in dielectric materials. Applications include three-dimensional optical storage [1–3] and fabrication of waveguides in glass [4–9]. The mechanisms responsible for the change of the index of refraction could vary, due to different laser parameters, such as energy and spot size, and material properties involved in these processes. Several mechanisms that may play a role have been reviewed recently [10]. The mechanism with regard to plastic stress and strain induced by the laser irradiation has not, however, been firmly established.

In this work, we propose that the change of the index of refraction is caused by laser-induced plastic residual strain and perform three-dimensional finite-element simulations to compute such changes. When laser pulses are focused inside a glass sample, the temperature of the irradiated region increases rapidly and the highest temperature is achieved at the center. A further increase of the temperature results in a conversion of the thermal expansion into plastic compressive strain, due to the fact that a free expansion of the heated zone is restricted by the surrounding cooler material. When the irradiated volume cools down, shrinkage of the heated material occurs. The thermal strain is totally canceled out after the sample completely cools down, but not the compressive strain generated during heating. We propose that this residual compressive strain is responsible for local densification and consequently the increase of the refractive index of the glass.

Several researches have been performed to study the stress and strain fields induced during laser processing of glass. A finite-element model was used to relate interferometric and birefringence data to the densification of fused silica under UV laser excitation [11]. In the experimental and numerical study of femtosecond laser-induced modifications in quartz, a strong compressive strain field was found surrounding the irradiated core [12]. The stress field inside the silica plates produced by femtosecond laser irradiation was revealed by investigating the topography of surface relaxation [13].

In this paper, we perform rigorous simulations of femtosecond laser heating of fused-silica glass and the subsequent stress and strain evolution using the finite-element method. Unlike most of the previous studies, which dealt with pulse energies higher than the threshold of optical breakdown, we consider a process in which the peak temperature in the glass is controlled below its softening point by using low-energy femtosecond laser pulses. Simulation results reveal the residual strain field and show that the microscale densification and local refractive-index changes occur in a region smaller than the area where the laser energy is absorbed.

## 2 Numerical calculation

Laser heating and stress and strain development in silica glass are calculated using a 3-D finite-element model. The localized heating by high-power laser pulses produces a non-uniform temperature field and this thermal load induces the residual stress and strain around the heated region. Therefore, both a thermal analysis and a stress and strain analysis are needed. These two analyses are treated as uncoupled since the heat dissipation due to deformation is negligible compared with the heat provided by the lasers. In an uncoupled thermo-mechanical model, a transient temperature field is obtained first in the thermal analysis and is then used as a thermal loading in the subsequent stress and strain analysis to obtain stress and strain distributions.

✉ Fax: +1-765/494-0539, E-mail: xxu@ecn.purdue.edu

The thermal analysis is based on solving the 3-D heat-conduction equation. The initial condition is that the whole domain is at room temperature (300 K). The boundary conditions are prescribed as the room temperature for all surfaces except the top surface, as shown in Fig. 1. The laser pulse is focused onto the top surface with a diameter of 2 μm, and the laser irradiation is treated as a surface heat flux. The laser intensity at the top surface is considered as having a Gaussian distribution in both $x$ and $y$ directions, which can be expressed as:

$$I_s(x, y, t) = I_0(t) \exp\left(-2\frac{(x-x_0)^2+(y-y_0)^2}{r^2}\right), \quad (1)$$

where $I_0(t)$ is the time-dependent laser intensity at the center of the laser pulse ($x = x_0$; $y = y_0$) and $r$ is the beam radius. The temporal profile of the laser intensity is treated as increasing linearly from zero to the maximum at 0.5 ps and then decreasing to zero at the end of the pulse at 1 ps. This is equivalent to considering the laser pulse as 0.5 ps FWHM. Practically, many femtosecond lasers have shorter pulse width, of the order of 100 fs. However, the time for energy to transfer from electrons to the lattice is much longer. It was estimated to be about 10 ps by measuring the damage threshold of fused silica as a function of laser pulse width [14]. Our calculations show that, at a given fluence, this lattice heating time does not change the peak temperature and the stress and strain as long as it is less than 10 ps.

The local radiation intensity $I(x, y, t)$ within the target is calculated considering exponential attenuation and surface reflection as

$$I(x, y, t) = (1 - R_f) I_s(x, y, t), \quad (2)$$

where $R_f$ is the optical reflectivity. Properties of the fused silica (Corning 7980) are used.

The thermal analysis is carried out for laser pulse energies of 0.2 nJ, 0.25 nJ, and 0.3 nJ, respectively. Note that this energy is the energy absorbed in a skin depth. In an actual process, the absorption of laser energy is low and the depth of absorption is long; both depend on the laser intensity. The maximum temperatures obtained are all lower than the softening point of fused silica (1858 K).

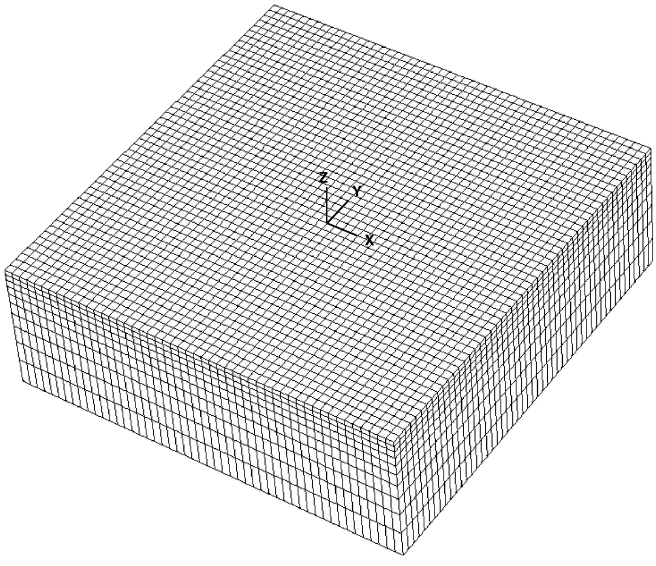


**FIGURE 1** Computational mesh ($x$ : 10 μm, $y$ : 10 μm, $z$ : 3 μm)

The transient temperature field obtained from the thermal analysis is used as the thermal loading to solve the quasi-static force equilibrium equations. The material is assumed to be linearly elastic–perfectly plastic. The von Mises yield criterion is used to model the onset of plasticity. The boundary conditions are zero displacement in the bottom plane and no displacement along the $z$ axis in the top surface, and all other surfaces are stress-free. Details of the equations to be solved have been described elsewhere [15].

Once the residual strain distribution is obtained, we can compute the change of the index of refraction, since it is proportional to the density as a first-order approximation. Kitamura et al. established a simple relationship to estimate the change of the index of refraction resulting from densification as [16]

$$\frac{\partial n}{n} = 0.4505\frac{\partial \varrho}{\varrho}, \quad (3)$$

where $n$ is the index of refraction of glass and $\delta\varrho/\varrho$ is the densification. The densification is related to the sum of the three diagonal linear strains as

$$\frac{\partial \varrho}{\varrho} = -\frac{\partial V}{V} = -\left(\frac{\partial u}{\partial x} + \frac{\partial v}{\partial y} + \frac{\partial w}{\partial z}\right). \quad (4)$$

The non-linear finite-element solver, ABAQUS (HKS, Inc., Pawtucket, RI), is employed for the simulation. The mesh used for the femtosecond pulsed laser simulation is shown in Fig. 1. The Cartesian coordinate system is attached to the computational domain, which has dimensions of 10 μm × 10 μm × 3 μm. The elements have uniform size (0.2 μm) along the $x$ and $y$ directions and the size is stretched along the $z$ direction. The total element number is 25 000. Mesh-refinement tests are performed by increasing the mesh density until calculations are independent of the mesh density. The same mesh is used for both thermal and stress analyses.

Temperature-dependent properties are used, including yield strength and Young's modulus. However, the strain-enhancement effect is neglected since data are not available.

## 3 Results and discussion

Temperature distributions along the $x$ direction at 1 ps are shown in Fig. 2. The laser pulse energy is 0.25 nJ and the pulse center is located at $x = y = 0$ μm. The peak temperature reaches a value of $T_{max} = 1438$ K at 1 ps. It can be estimated that the laser-heated region is around 1.6 μm in radius on the top surface, slightly larger than the diameter of the focused laser spot, which is 2 μm. We also calculate the temperature distribution induced by laser pulses with pulse widths of 100 fs, 10 ps, and 1 ns, respectively, using the same laser energy. As shown in Fig. 3, the peak temperatures induced by 100-fs and 10-ps pulses are about the same as that by the 1-ps pulse. But, for the 1-ns pulse, the peak temperature is only 986 K and is much lower than those obtained from shorter pulses. This is because the heat-diffusion

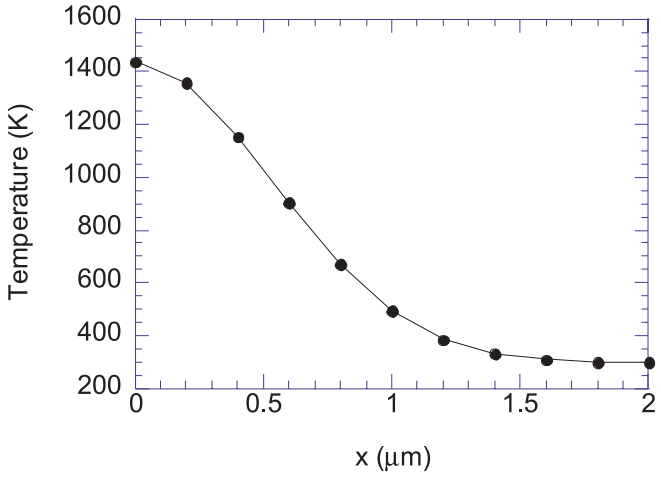


**FIGURE 2** Temperature profile along the $x$ direction (laser pulse energy 0.25 nJ, pulse width 1 ps, laser spot size 2 μm)

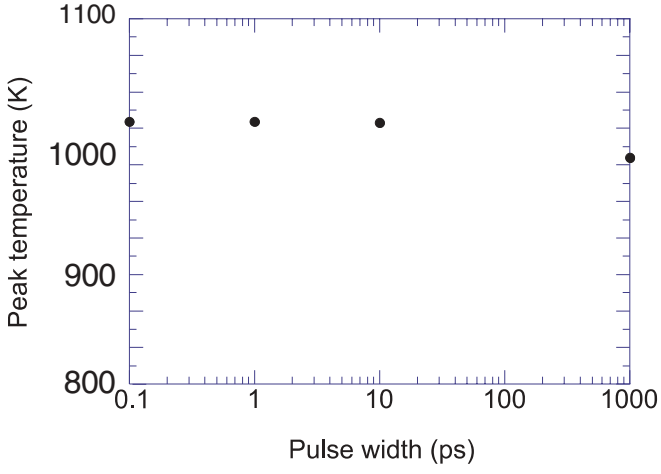


**FIGURE 3** Peak temperature induced by different laser pulse widths (laser pulse energy 0.6 nJ, laser spot size 4 μm)

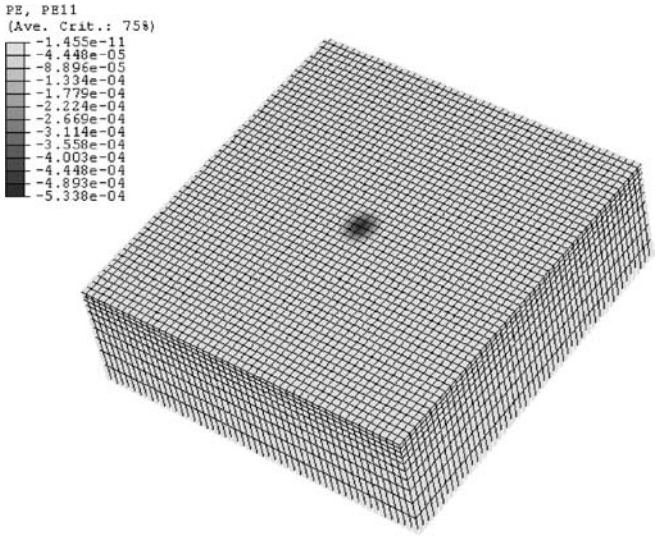


**FIGURE 4** Residual strain $\varepsilon_{xx}$ distribution (laser pulse energy 0.25 nJ, pulse width 1 ps, laser focusing size 2 μm)

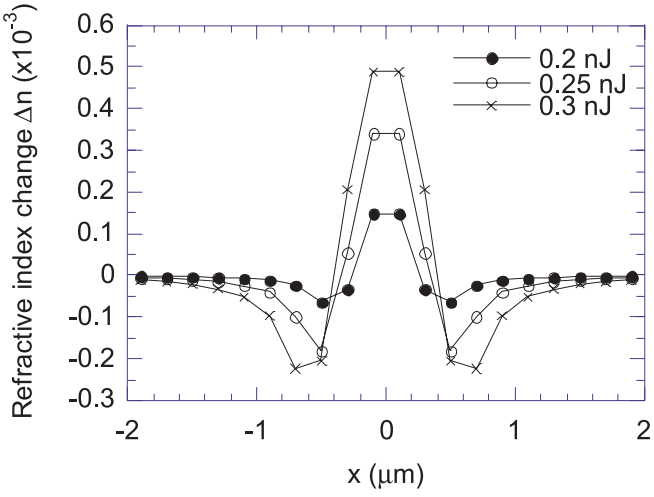


**FIGURE 5** Change of index of refraction of fused silica irradiated by a single ultra-fast laser pulse (laser pulse energy 0.2, 0.25, and 0.3 nJ, pulse width 1 ps, laser spot size 2 μm)

depth within a few ps is almost negligible. It is found that temperature profiles of the 100-fs laser pulse are exactly the same as those of the 1-ps laser pulse except that the peak temperature is reached at 132 fs instead of 1 ps. However, as explained previously, even for a 100-fs femtosecond laser pulse, it still takes picoseconds for energy to be coupled to the lattice. With the same peak temperature, the laser-induced strain and stress development is determined by the cooling rate, which is the same in the two cases. Therefore, it is not so critical to know exactly when the peak temperature is obtained.

The distribution of the residual strain, $\varepsilon_{xx}$, on the surface is shown in Fig. 4. It can be seen that the residual strain is compressive with the maximum value at the core of the irradiated area. The compressive strain indicates densification of the glass, and the area of compressive strain is smaller than the laser spot size, 2 μm. The change of the index of refraction is calculated using (3) and (4), and is shown in Fig. 5. Due to the symmetry of the model, only the change along the $x$ direction is plotted. Three different laser pulse energies are used in the calculations. As shown in Fig. 5, the change of the index of refraction increases with the pulse energy. The maximum value of $\Delta n$ is $0.5 \times 10^{-3}$ for the 0.3-nJ pulse, while it is only about $0.15 \times 10^{-3}$ for the 0.2-nJ pulse. The size of the densified region where the index of refraction increases can be estimated to be around 1 μm, which is one-half of the laser spot size.

Figure 6 shows the diameters of the densification zone in glass induced by different laser spot sizes but where the peak temperature obtained during heating is kept the same. It is found that the diameters of the strained regions are all about one-half of the laser spot sizes. This small size is first due to the negligible heat diffusion during the short period of time. Further, the plastic strain is produced only in the near-center region, since generation of plastic strain is highly temperature dependent due to the temperature-dependent stress–strain relation (similar to the narrowing of the absorption profile in a non-linear optical absorption process). These two effects are responsible for the localized change of the index of refraction as compared with the laser-heated area.

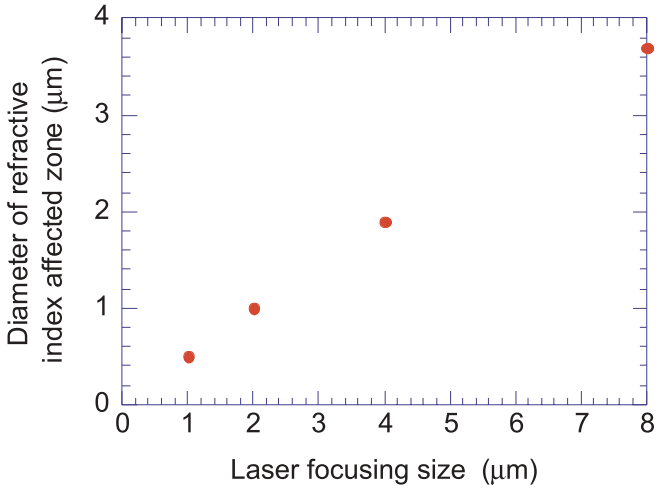


**FIGURE 6** Diameter of densification zone inside the fused glass induced by different spot sizes but the same peak temperature ($T_{max} = 1438$ K)

Lastly, it is noticed that the interaction between the femtosecond laser pulse and the glass is a multi-photon process. Considering the multi-photon effect, the region where the laser pulse is absorbed as defined by the Gaussian distribution function is a factor of $\sqrt{n}$ smaller than the laser beam diameter, where $n$ is the number of photons involved in the absorption process. For most glasses, their band gaps are more than twice the energy of the photons from a Ti : sapphire laser (1.55 eV); therefore, a three or more photon absorption process occurs. For a three-photon process, the absorption profile is 1.73 times smaller than the laser spot. Or, in this calculation, the 2-μm-diameter region where the laser energy is absorbed originates from a 3.46-μm-diameter laser spot. Our computation results show that the change of the index of refraction is confined in a region of 1 μm when the laser pulse is absorbed in a 2-μm spot. This indicates that a 3.46-μm laser beam can produce a change of index of refraction within a 1-μm-diameter spot.

## 4 Summary

Femtosecond laser processing of fused silica is simulated by using the finite-element method. Calculations show that a localized change of index of refraction occurs in an area smaller than the laser-heated region. The densification zone is about one-half of the region where the laser energy is absorbed. This densification zone is further reduced if the multi-photon absorption effect is considered. Thus, we conclude that the laser-induced strain field, as well as the multi-photon absorption effect, is responsible for the localized change of the index of refraction of the glass.

**ACKNOWLEDGEMENTS** Support of this work by the National Science Foundation (DMI-9908176) is gratefully acknowledged.

## REFERENCES

1 E.N. Glezer, M. Milosavljevic, L. Huang, R.J. Finlay, T.-H. Her, J.P. Callan, E. Mazur: Opt. Lett. **21**, 2023 (1996)
2 K. Yamasaki, S. Juodkazis, M. Watanabe, H.B. Sun, S. Matsuo, H. Misawa: Appl. Phys. Lett. **76**, 1000 (2000)
3 J.R. Qiu, K. Miura, K. Hirao: Jpn. J. Appl. Phys. Part 1 **37**, 2263 (1998)
4 K.M. Davis, K. Miura, N. Sugimoto, K. Hirao: Opt. Lett. **21**, 1729 (1996)
5 K. Miura, J.R. Qiu, H. Inouye, T. Mitsuyu, K. Hirao: Appl. Phys. Lett. **71**, 3329 (1997)
6 D. Homoelle, S. Wielandy, A.L. Gaeta, N.F. Borrelli, C. Smith: Opt. Lett. **24**, 1311 (1999)
7 C.B. Schaffer, A. Brodeur, J.F. Garcia, E. Mazur: Opt. Lett. **26**, 93 (2001)
8 M. Will, S. Nolte, B.N. Chichkov, A. Tunnermann: Appl. Opt. **41**, 4360 (2002)
9 A.M. Streltsov, N.F. Borrelli: J. Opt. Soc. Am. B **19**, 2496 (2002)
10 C.B. Schaffer, J.F. Garcia, E. Mazur: Appl. Phys. A **76**, 351 (2003)
11 N.F. Borrelli, C. Smith, D.C. Allan, T.P. Seward III: J. Opt. Soc. Am. B **14**, 1606 (1997)
12 T. Gorelik, M. Will, S. Nolte, A. Tuennermann, U. Glatzel: Appl. Phys. A **76**, 309 (2003)
13 B. Poumellec, L. Sudrie, M. Franco, B. Prade, A. Mysyrowicz: Opt. Express **11**, 1070 (2003)
14 B.C. Stuart, M.D. Feit, S. Herman, A.M. Rubenchik, B.W. Shore, M.D. Perry: Phys. Rev. B **53**, 1749 (1996)
15 G. Chen, X. Xu: J. Manuf. Sci. Eng. **123**, 66 (2001)
16 N. Kitamura, Y. Toguchi, S. Funo, H. Yamashita, M. Kinoshita: J. Non-Cryst. Solids **159**, 241 (1993)